

Vortex Filament Dynamics

Jim Thomas

August 16, 2015

1 Introduction

Formation of large coherent vortices is a recurring theme in two-dimensional turbulence investigations [1]. DNS simulations and lab experiments have demonstrated this time and again. Once these large vortices form, like-signed vortices merge together in an inelastic process. During this merger process filamentation occurs leading to the formation of thin strips of vorticity. While some filaments remain attached to the large coherent vortices others are expelled during the merger and remain detached from the large vortices. Under normal conditions one would naturally expect these filaments to be unstable to perturbations, the growth of instabilities leading to roll up of these filaments. But surprisingly, it has been demonstrated that in the presence of other coherent vortices, the rolling up of these filaments is inhibited [2]. The strong external shearing and straining fields prevents the rolling up of these filaments. As a result, the filaments form a characteristic feature of fully developed 2D turbulence. This work aims to capture the dynamics of these filaments using a simple new model. An integro-differential equation is derived for this purpose, which is then solved for a variety of cases.

In Sec. 2 derivation of the relevant equations and some of its properties are discussed. Sec. 3 involves studying the effect of disturbances on filaments and response of filaments to externally imposed velocity fields. Possibility of equilibrium states for filaments in the presence of external fields is discussed in Sec. 4 . Some filament-point vortex and filament-filament interactions are investigated in Sec. 5 .

2 Mathematical Model

A vortex filament (VF hereafter) is a very thin strip of vorticity in the $x - y$ plane. The small thickness assumption will be used to characterize the filament by its center line curve. Mass (area) conservation and material transport of vorticity are used to describe variation in local thickness and vorticity.

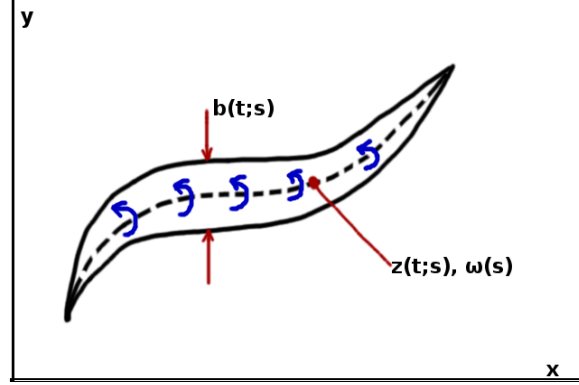


Figure 1: A vortex filament: $z(s,t)$ is a curve in the complex plane parametrised by s , varying with time, and $b(s,t)$ is the local filament thickness.

2.1 Derivation of the VF equation

The VF equation is derived from first principles here.

Vorticity at any point is

$$\boldsymbol{\omega} = \nabla \times \boldsymbol{v}$$

$$\nabla \cdot \boldsymbol{v} = 0 \quad \Rightarrow \quad \boldsymbol{v} = \hat{\boldsymbol{z}} \times \nabla \psi .$$

Combining above two equations gives

$$\Delta \psi = \omega$$

If vorticity field is compact, this can be uniquely solved to get

$$\psi(\boldsymbol{x}) = \frac{1}{2\pi} \int_{\boldsymbol{x}' \in \mathbb{R}^2} \omega(\boldsymbol{x}') \ln |\boldsymbol{x} - \boldsymbol{x}'| d\boldsymbol{x}'$$

which leads to

$$\boldsymbol{v}(\boldsymbol{x}) = \frac{1}{2\pi} \int_{\boldsymbol{x}' \in \mathbb{R}^2} \frac{\hat{\boldsymbol{z}} \times (\boldsymbol{x} - \boldsymbol{x}')}{|\boldsymbol{x} - \boldsymbol{x}'|^2} \omega(\boldsymbol{x}') d\boldsymbol{x}'$$

This is the 2D version of the infamous Biot- Savart law.

Using small thickness approximation, we write $d\boldsymbol{x}' = b(s')dl(s')$, $\omega = \gamma(s')$

This is analogous to thin airfoil approximation in aerodynamics [3].

Thus, self-induced velocity of the filament at any point is

$$\boldsymbol{v}(\boldsymbol{x}, t) = \frac{1}{2\pi} \int_L \gamma(s') \frac{\hat{\boldsymbol{z}} \times (\boldsymbol{x}(s, t) - \boldsymbol{x}(s', t'))}{|\boldsymbol{x}(s, t) - \boldsymbol{x}(s', t)|^2} b(s', t) dl(s')$$

The sum of this and the external velocity is the total velocity at any point on the filament, i.e.

$$\frac{\partial \mathbf{x}(s, t)}{\partial t} = \mathbf{U}(\mathbf{x}(s), t) + \frac{1}{2\pi} \int_L b(s', t) \gamma(s') \frac{\hat{\mathbf{z}} \times (\mathbf{x}(s, t) - \mathbf{x}(s', t))}{|\mathbf{x}(s, t) - \mathbf{x}(s', t)|^2} dl(s')$$

Or in complex variable notation,

$$\frac{\partial \mathbf{z}^*(s, t)}{\partial t} = \mathbf{U}^*(\mathbf{z}) + \frac{1}{2\pi i} \int_L \frac{b(s', t) |\mathbf{z}_s(s', t)| \gamma(s')}{\mathbf{z}(s, t) - \mathbf{z}(s', t)} ds'$$

where $\mathbf{z} = x + iy$

To close the system, we need an evolution equation for thickness. This can be derived by demanding local area conservation of the VF.

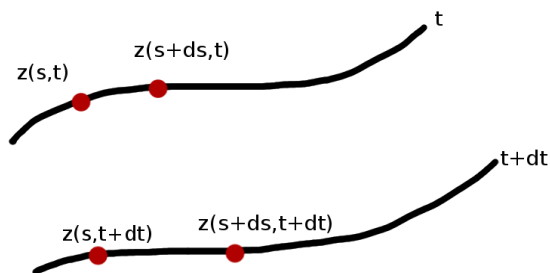


Figure 2: Centerline curve of a VF at two different times

On demanding that local area remains same at t and $t + \delta t$

$$b(s + \delta s/2, t) |\mathbf{z}(s + \delta s, t) - \mathbf{z}(s, t)| = b(s + \delta s/2, t + \delta t) |\mathbf{z}(s + \delta s, t + \delta t) - \mathbf{z}(s, t + \delta t)|$$

$$b(s, t) |\mathbf{z}_s(s, t) \delta s| = (b(s, t) + \delta t b_t(s, t)) |\mathbf{z}_s(s, t) \delta s + \mathbf{z}_{st}(s, t) \delta s \delta t| + O(\delta s^2)$$

$$\frac{1}{b} \frac{\partial b}{\partial t} + \frac{1}{2|\mathbf{z}_s|^2} \frac{\partial |\mathbf{z}_s|^2}{\partial t} = 0$$

After some simplifications, this yields

$$b(s, t) |\mathbf{z}_s(s, t)| = b(s, 0) |\mathbf{z}_s(s, 0)| = b^0(s) |\mathbf{z}_s^0|$$

This is a remarkable result since it implies that thickness in this model is slaved to the curve. As a consequence, one need not solve for the thickness simultaneously with the curve points. Once the curve is known, thickness can be calculated and updated.

The final equation is then

$$\frac{\partial \mathbf{x}(s, t)}{\partial t} = \mathbf{U}(\mathbf{x}) + \frac{1}{2\pi} \int_L b^0(s') |\mathbf{x}_s^0| \gamma(s') \frac{\hat{\mathbf{z}} \times (\mathbf{x}(s, t) - \mathbf{x}(s', t))}{|\mathbf{x}(s, t) - \mathbf{x}(s', t)|^2} ds'$$

which is in complex notation

$$\frac{\partial \mathbf{z}^*(s, t)}{\partial t} = \mathbf{U}^*(\mathbf{z}) + \frac{1}{2\pi i} \int_L \frac{b^0(s') |\mathbf{z}_s^0| \gamma(s')}{\mathbf{z}(s, t) - \mathbf{z}(s', t)} ds' \quad (1)$$

This formulation can be extended to include multiple filaments as given below:

$$\begin{aligned} \frac{\partial \mathbf{x}_i(s_i, t)}{\partial t} = & \mathbf{U}(\mathbf{x}_i) \\ & + \frac{1}{2\pi} \int_{L_i} b_i^0(s'_i) |\mathbf{x}_{i s'_i}^0| \gamma_i(s'_i) \frac{\hat{\mathbf{z}} \times (\mathbf{x}_i(s_i, t) - \mathbf{x}_i(s'_i, t))}{|\mathbf{x}_i(s_i, t) - \mathbf{x}_i(s'_i, t)|^2} ds'_i \\ & + \sum_j \frac{1}{2\pi} \int_{L_j} b_j^0(s'_j) |\mathbf{x}_{j s'_j}^0| \gamma_j(s'_j) \frac{\hat{\mathbf{z}} \times (\mathbf{x}_i(s_i, t) - \mathbf{x}_j(s'_j, t))}{|\mathbf{x}_i(s_i, t) - \mathbf{x}_j(s'_j, t)|^2} ds'_j \end{aligned}$$

The last summation over all other filaments is the mutual interaction term.

Analogous to Contour Dynamics (CD) we shall call this model Filament Dynamics (FD hereafter)

As a special singular limit, let $b \rightarrow 0, \gamma \rightarrow \infty$ holding $b\gamma$ fixed and $L \rightarrow \infty$. Then (1) reduces to:

$$\frac{\partial \mathbf{z}^*(s, t)}{\partial t} = \frac{1}{2\pi i} \int_{-\infty}^{\infty} \frac{d\Gamma(s')}{\mathbf{z}(s, t) - \mathbf{z}(s', t)}$$

This is the Birkhoff-Rott equation used to model the evolution of a vortex sheet [4,5].

2.2 Conservation laws for self interacting filament ($\mathbf{U}=\mathbf{0}$)

Equation (1) has a Hamiltonian formulation.

Hamiltonian,

$$H[\mathbf{x}] = -\frac{1}{2\pi} \int_s \int_{s'} b^0(s) |\mathbf{x}_s^0| \gamma(s) b^0(s') \gamma(s') |\mathbf{x}_s^0(s')| \ln |\mathbf{x}(s, t) - \mathbf{x}(s', t)| ds' ds$$

Thus, (1) can be written as Hamilton's equations

$$\begin{aligned} \frac{\partial x}{\partial t} &= \frac{1}{\zeta} \frac{\delta H}{\delta y} \\ \frac{\partial y}{\partial t} &= -\frac{1}{\zeta} \frac{\delta H}{\delta x} \end{aligned}$$

where $\zeta = \gamma(s)b^0(s) |\mathbf{x}_s^0(s)|$

Thus, the Hamiltonian (Energy) is an invariant of the system, i.e. $H_t = 0$

The Hamiltonian can be modified to include the effect of external velocity field using the stream function.

An invariant center of vorticity $\bar{\mathbf{x}}$ can be defined for a VF such that

$$\oint_L b^0(s') |\mathbf{x}_{s'}^0| \gamma(s') \frac{\hat{z} \times (\bar{\mathbf{x}} - \mathbf{x}(s', t))}{|\bar{\mathbf{x}} - \mathbf{x}(s', t)|^2} ds' = 0$$

The center of vorticity $\bar{\mathbf{x}}$, is the point where the velocity induced by the whole filament is zero.

Equation (1) conserves angular momentum.

Angular Momentum,

$$L = \oint_s b^0(s) |\mathbf{x}_s^0(s)| \gamma(s) |\mathbf{x}(s, t)|^2 ds$$

2.3 Numerical solutions

Examples are calculated by a numerical scheme in which the VF is discretized into rectangular strips with N points on it. The system of $2N$ equations are then solved using RK-4. The integral is replaced with a desingularised summation [6]

$$\sum_j \frac{1}{|\mathbf{x}_i - \mathbf{x}_j|^2 + \delta^2}$$

with midpoints between two points used to evaluate the sum. Thickness is at the midpoint between two points. After each time step (n), the thickness is updated using

$$b_j^{n+1} l_j^{n+1} = b_j^n l_j^n$$

3 Effect of Disturbances on VFs

It is well known that thin strips of vorticity are unstable to disturbances and tend to roll up. Here we test this using our model. We study two cases: a parabolic VF and a circular VF.

A parabolic VF has thickness variation

$$b(s) = b_{max}(1 - s^2), \quad s \in [-1, 1]$$

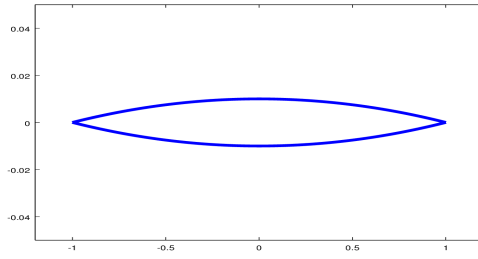


Figure 3: A parabolic VF

This is now disturbed by a finite amplitude sinusoidal perturbation and allowed to evolve. In the configuration that we study, maximum thickness, $b_{max} = 10^{-5}$
The initial and long time states are shown below:

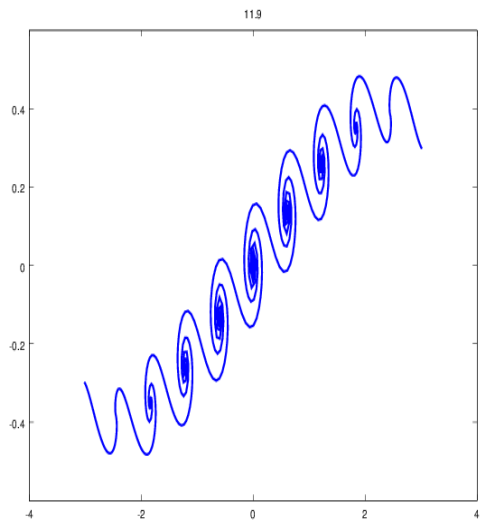
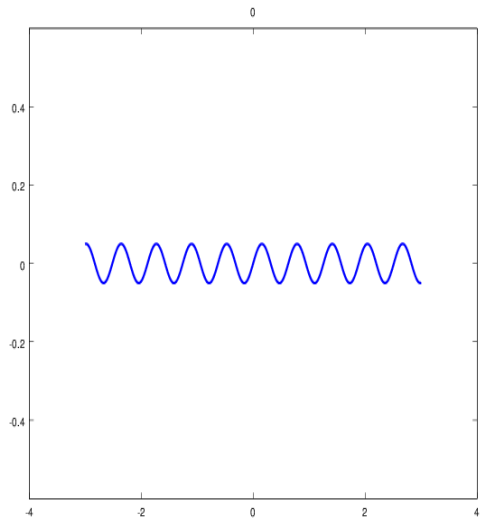


Figure 4: Initial and long time state of a perturbed parabolic VF

The second case we study is a slightly perturbed circular VF. The circular VF is of constant thickness, $b = .02$

The initial and long time states are shown below:

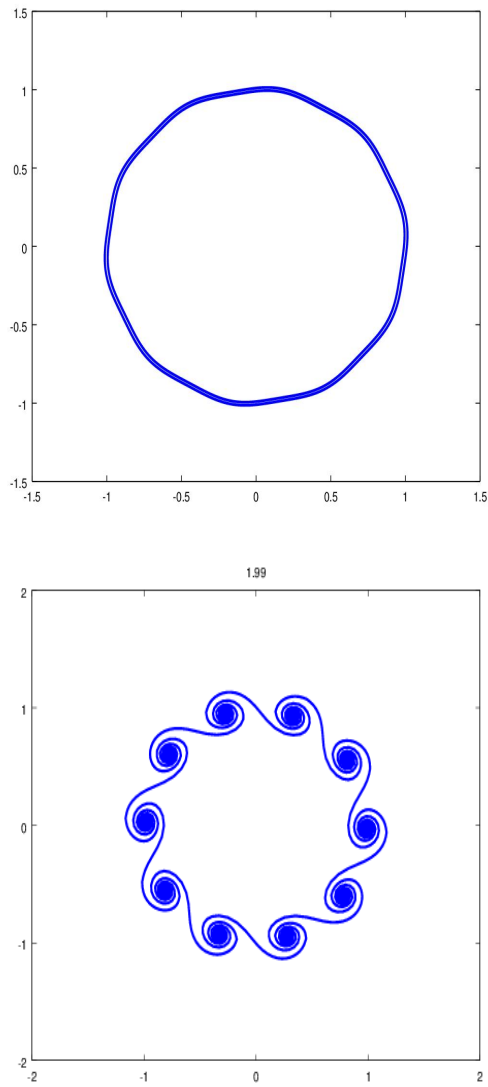
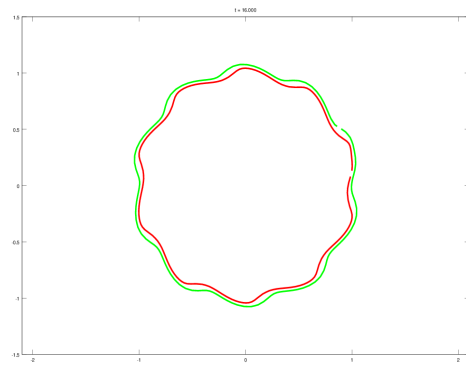
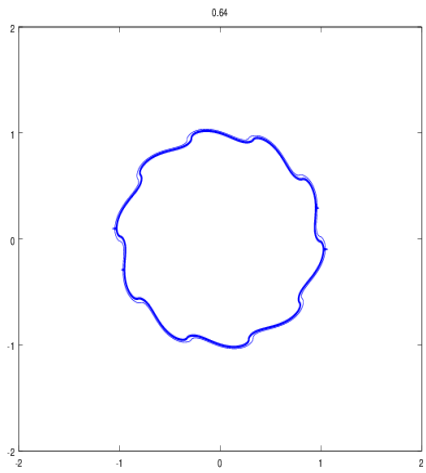
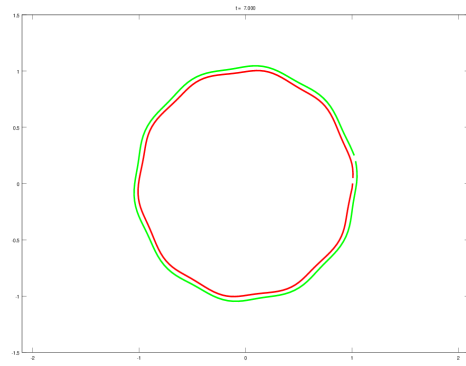
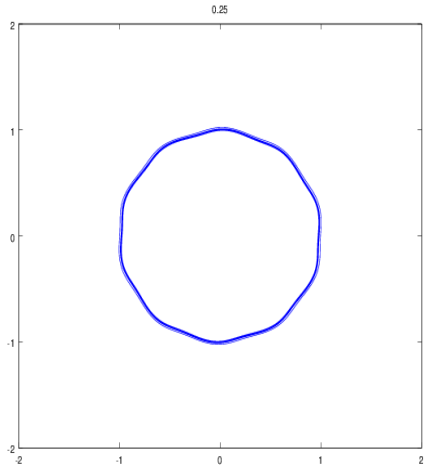
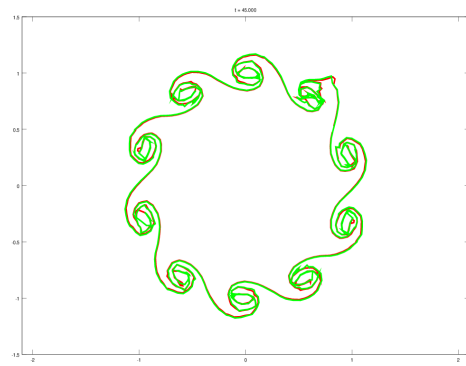
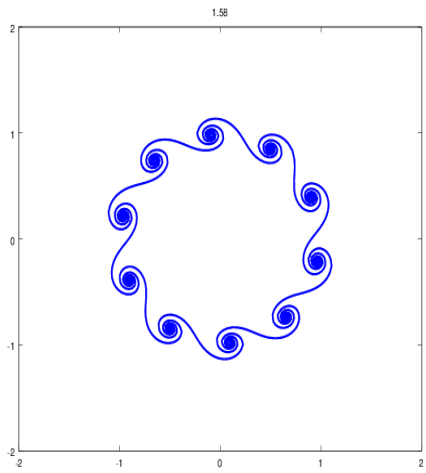
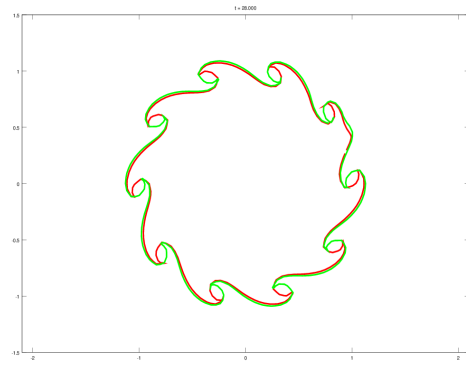
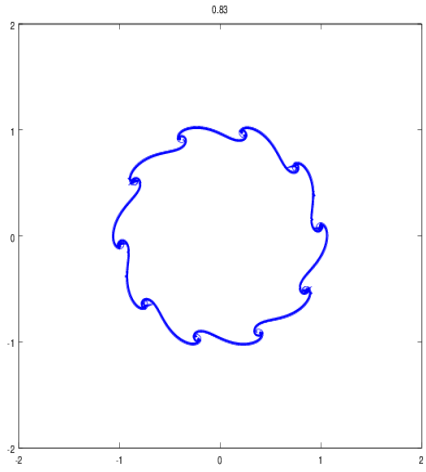


Figure 5: Initial and long time state of a perturbed circular VF

Thus VFs, as expected do roll up on being disturbed. For the case of a slightly disturbed circular VF, we compare this model with a Contour Dynamics calculation. Various stages of evolution are as shown:





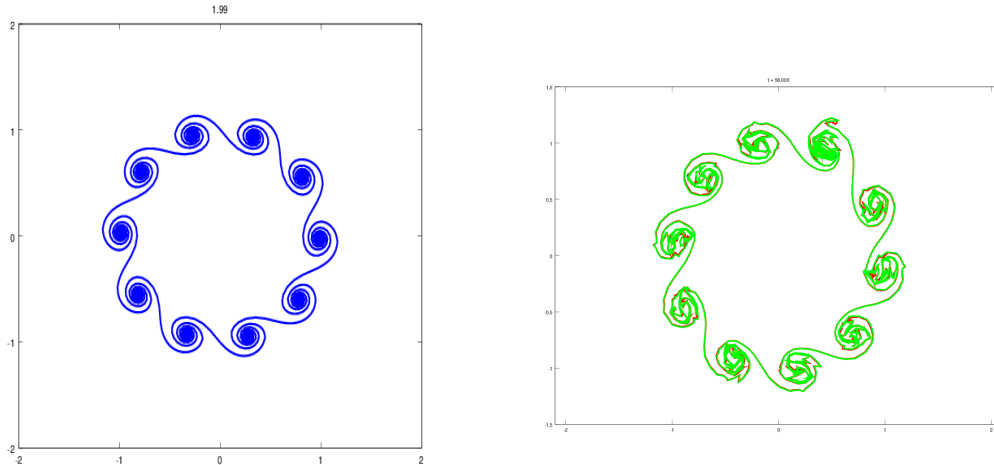


Figure 6: Comparison between FD and CD

Note that disturbances propagate and grow in both models. Thickening happens in certain regions leading to the formation of beads of vorticity. However, the FD model is unable to maintain regions of constant vorticity as CD and it rolls up into a spiral in the final stages as seen above.

3.1 Shape of VFs and their influence on dynamics

The dynamics of VFs depend a lot on their shapes. It is seen that an elliptical VF ($(\frac{x}{a})^2 + (\frac{y}{b})^2 = 1$) rotates without change of shape.

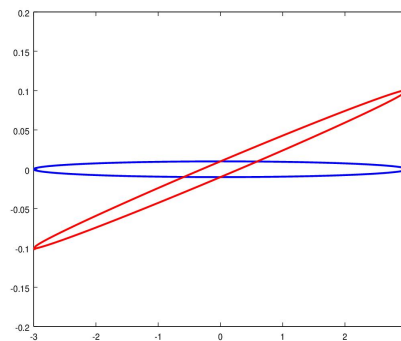


Figure 7: Elliptic VF-red is initial configuration and blue is state after a small time

Hyper-ellipses ($(\frac{x}{a})^n + (\frac{y}{b})^n = 1, n > 2$) rotate with their tips leading the main body of rotation.

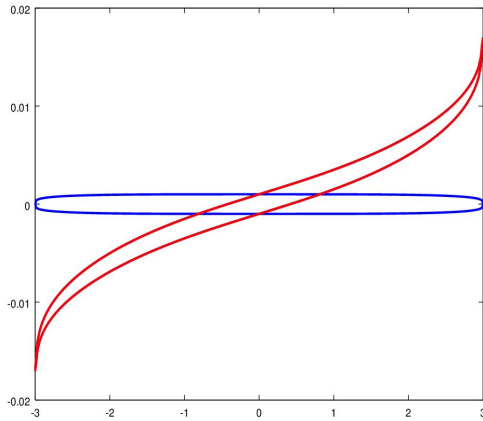


Figure 8: Hyper-elliptic VF-red is initial configuration and blue is state after a small time

A parabolic filament ($b = b_{max}(1 - s^2)$) rotates with its tip lagging behind the main body of rotation.

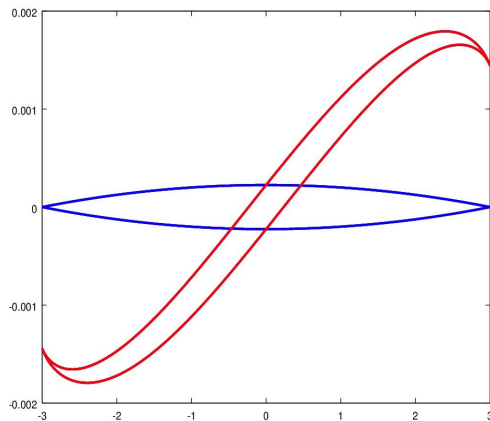


Figure 9: Parabolic VF-red is initial configuration and blue is state after a small time

Further investigations indicate that sharper filament tips tend to lag while blunter filament tips have a tendency to lead the main body of the filament.

3.2 Effect of external velocity field on VFs

Here we impose an external velocity field and study the response of the VF. The previous case of perturbed parabolic VF is used but now a velocity field equivalent to the presence of a point vortex at $(0,3)$ is imposed. i.e., $v_r = 0$, $v_\theta = \frac{\Gamma}{2\pi|\mathbf{x}-3\hat{\mathbf{y}}|}$

Two cases are considered. Case of weak external field ($\Gamma / (2\pi b_{max} L \gamma) \ll 1$) and strong external field ($\Gamma / (2\pi b_{max} L \gamma) \gg 1$) as shown below:

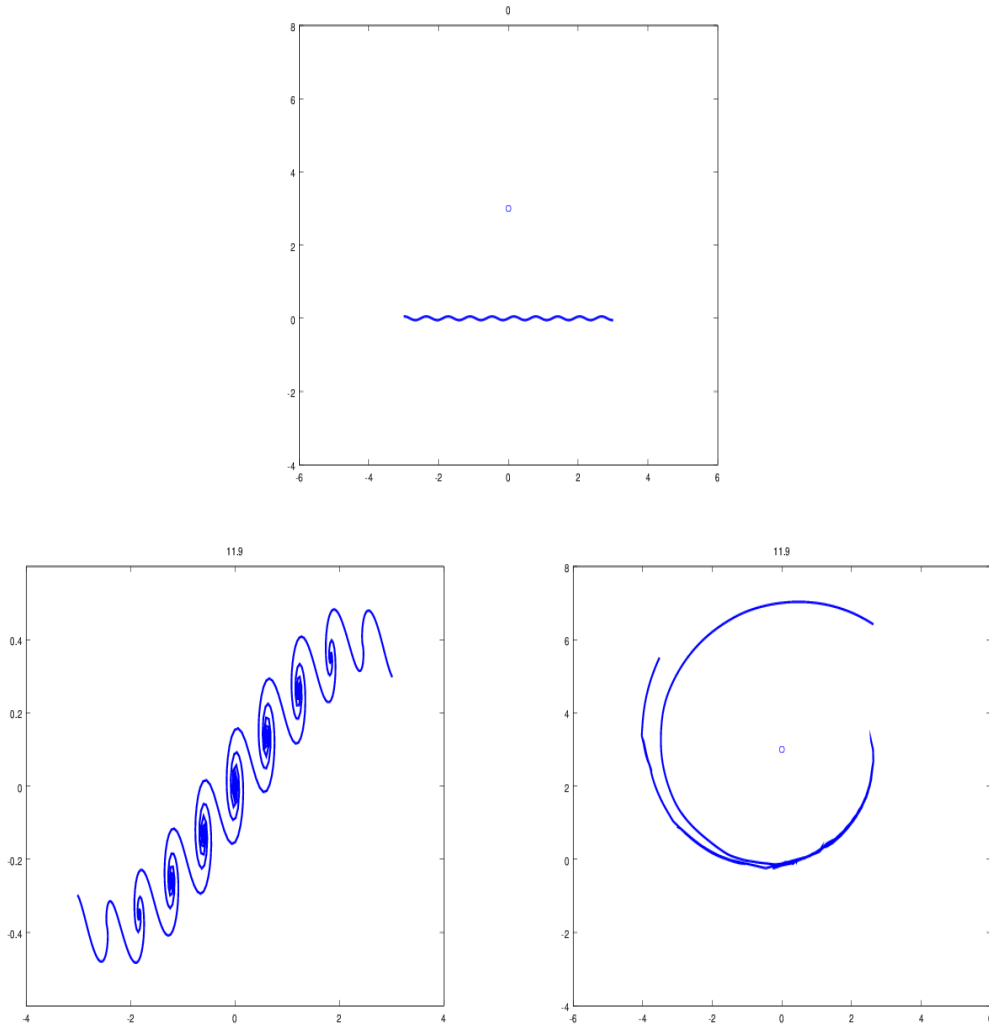


Figure 10: Counterclockwise from top: Initial state, long time state in the absence of external field, long time state in the presence of external field

In the case of weak external velocity, rolling up of the VF occurs as expected. But in the presence of strong external velocity field, the filament is extremely stretched out and flattened, preventing all rolling up activities.

Further numerical experiments indicate that a strong external field can stretch the VF so as to prevent rolling up from occurring. On the other hand, a weak external flow is unable to impact the VF. This leads to the natural question of equilibrium. Are there critical velocity fields that can hold the whole VF in equilibrium?

4 Equilibrium states of VFs

The relevant equations for equilibrium states are

$$\mathbf{U}^*(\mathbf{z}) + \frac{1}{2\pi\iota} \int_L \frac{b(s')\gamma(s')}{\mathbf{z}(s) - \mathbf{z}(s')} |z_s(s')| ds' = 0$$

Closed filaments

For the class of closed filaments, a circular filament of constant thickness and vorticity is in self equilibrium, i.e. $\mathbf{U}=0$. This is easily verified by using $z = e^{i\theta}$ to evaluate the integral.

Open filaments

Consider straight filaments placed on the x -axis with constant vorticity along the curve. Thus $z = s$ is the equation of the VF. We prescribe various thickness distributions and find the corresponding flow fields based on the equation:

$$\mathbf{U}(s) = \frac{\iota\gamma}{2\pi} \int_L \frac{b(s')}{s - s'} ds' \quad (2)$$

1. $b(s) = b_{max} \sqrt{1 - (s/a)^2}$

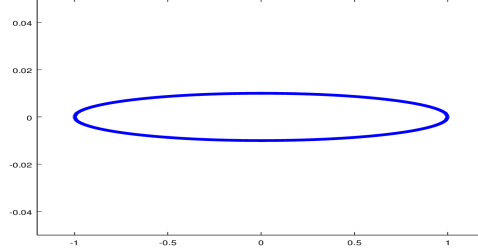


Figure 11:

This is an elliptic thickness variation as shown. For this $b(s)$, the critical velocity field is

$$u = ky, \quad v = -kx \Rightarrow \omega = -2k \quad (k = \gamma b_{max}/2a)$$

This is a flow with constant vorticity that can hold an elliptic VF in equilibrium. Half the vorticity of this external field is exactly the rotation rate of an elliptic VF.

Consider an ellipse $\frac{x^2}{a^2} + \frac{y^2}{c^2} = 1$

In the filament approximation, we obtain the rotation rate as

$$\Omega_f = \gamma\lambda$$

where $\lambda = \frac{c}{a}$ is the aspect ratio

If we had an elliptic patch of constant vorticity [7],

$$\Omega = \gamma \frac{\lambda}{(1 + \lambda)^2}$$

If $\lambda \ll 1$, binomial expansion gives $\Omega \sim \Omega_f + O(\lambda^2)$.

Thus, in the filament approximation, the ellipse tends to rotate faster, the difference being $O(\lambda)$.

2. $b(s) = b_{max}(1 - s^2)^{3/2}$

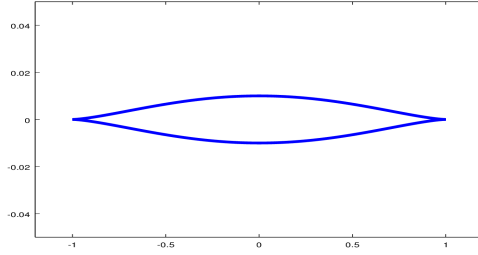


Figure 12:

The critical velocity field is

$$u = k_o \left(\frac{3}{2}y + y^3 - 3x^2y \right), \quad v = -k_o \left(\frac{3}{2}x - x^3 + 3y^2x \right)$$

3. $b(s) = b_{max}(1 - s^2)$

This is a parabolic thickness variation.

$$b(s) = b_{max}(1 - s^2)$$

The critical velocity field in complex notation is

$$\mathbf{U} = -k_p \left((1 - z^2) \ln \frac{1+z}{1-z} + 2z \right)$$

The k_i 's are constants that depend on the central region thickness of the filament and similar other parameters.

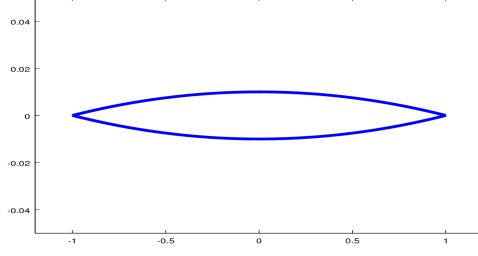


Figure 13:

Stability of equilibria

Here the stability of equilibria of VF is tested. We shall consider small local perturbations on an elliptic VF and study its evolution.

The disturbance equations are:

$$\frac{\partial \widehat{\mathbf{z}}^*(s, t)}{\partial t} = \widehat{\mathbf{U}}^*(\mathbf{z}_e, \widehat{\mathbf{z}}) - \frac{1}{2\pi\iota} \int_L \frac{b_e(s') |\mathbf{z}_e(s')| \gamma^0(s')}{(\mathbf{z}_e(s) - \mathbf{z}_e(s'))^2} (\widehat{\mathbf{z}}(s, t) - \widehat{\mathbf{z}}(s', t)) ds'$$

Consider small perturbation on a straight elliptical filament with constant vorticity distribution in an equilibrium flow field. Then $\mathbf{z}_e = s$, $\mathbf{U} = \iota\beta\mathbf{z}$, $b_e(s) = \sqrt{1 - s^2}$ and after dropping $\widehat{\ } ' s$ leads to

$$(\mathbf{z}_t(s, t) + \iota\beta\mathbf{z})^* = -\frac{\gamma^0}{2\pi\iota} \int_{-a}^a b_0 \frac{\sqrt{1 - (s'/a)^2}}{(s - s')^2} (\mathbf{z}(s, t) - \mathbf{z}(s', t)) ds'$$

Setting $s = a\xi$

$$(\mathbf{z}_t + \iota\beta\mathbf{z})^* = -\frac{\beta}{\pi\iota} \int_{-1}^1 \frac{\sqrt{1 - \xi'^2}}{(\xi - \xi')^2} (\mathbf{z}(\xi, t) - \mathbf{z}(\xi', t)) d\xi'$$

where $\beta = \gamma^0 b^0 / (2a)$ which can be written as

$$(\mathbf{z}_t + \iota\beta\mathbf{z})^* = -\frac{\beta}{\pi\iota} F[\mathbf{z}]$$

Looking for solutions in terms of the normal modes,

$$\mathbf{z} = \sum A_n e^{\sigma_n t} \phi_n$$

where ϕ_n satisfies $F[\phi_n] = \lambda_n \phi_n$ and for the functional $F[\mathbf{z}]$, one can show that the eigenvalues are $\lambda_n = n\pi$

Thus,

$$\sigma_n = \pm\beta\sqrt{n^2 - 1}$$

which implies that all modes except $n = 0$ and 1 are unstable.

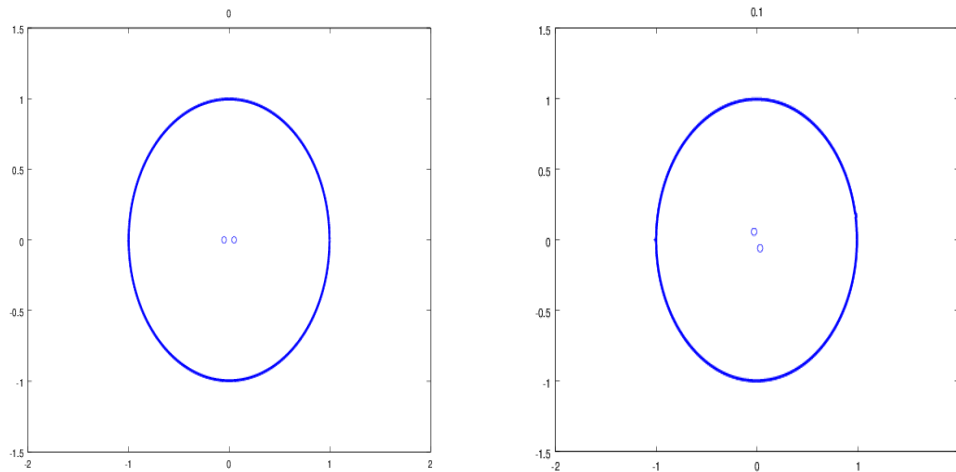
Hence, in spite of having critical velocity fields being capable of holding the whole VF in equilibrium, these states are in general unstable.

5 Interaction experiments

Here we study two types of interactions with point vortices and VF-VF interaction.

5.1 Interaction with point vortices

The original VF equation can be modified to include the effects of point vortices. Here we place two point vortices symmetrically inside a circular VF. Initially the point vortices just rotate about the center of the circular VF. Due to numerical instabilities the center of point vortices slightly shifts from the center of the circular VF. Once this happens, the point vortices destabilizes the VF by increasing thickness (hence vorticity) in certain regions at the expense of other regions and the region then rolls up as shown in the figures above.



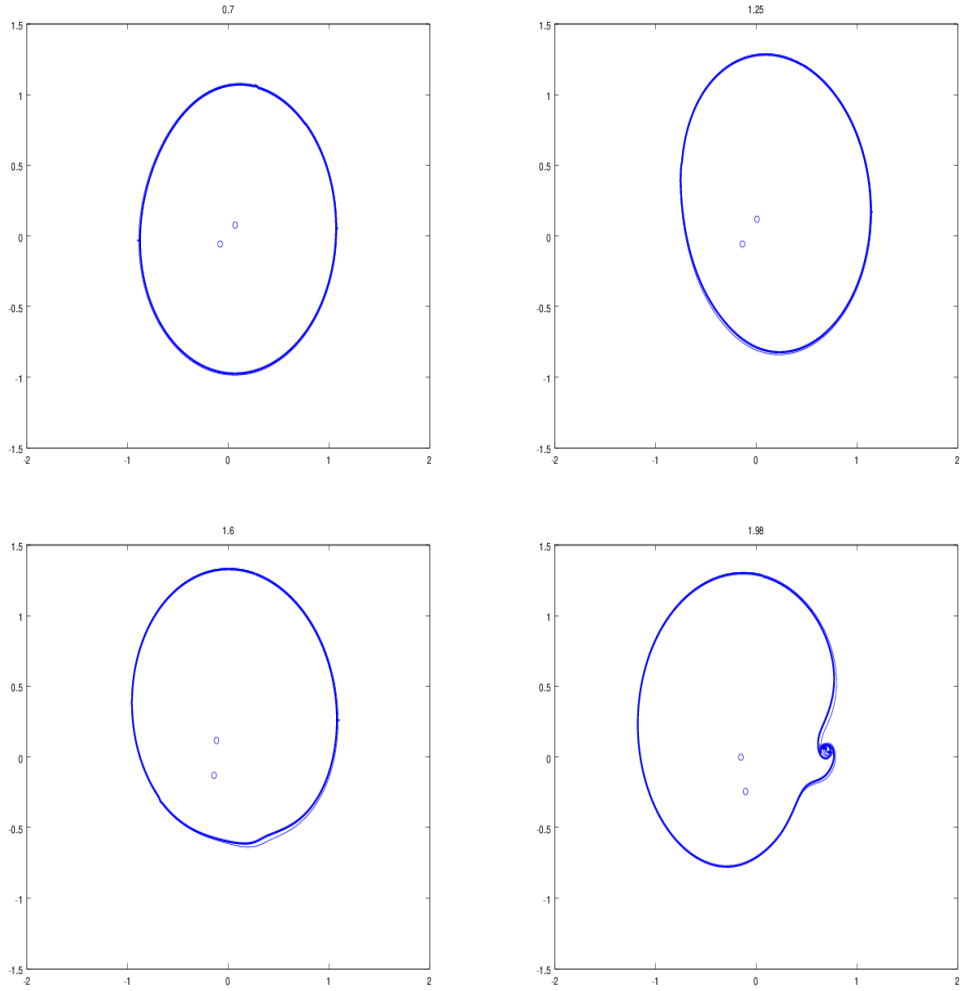
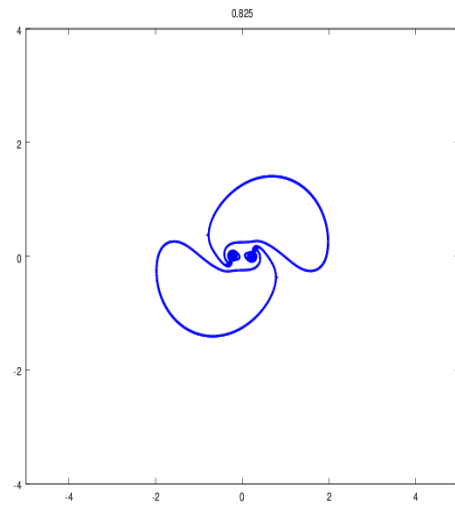
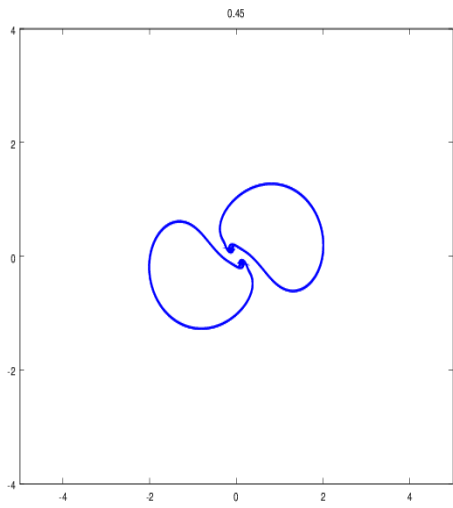
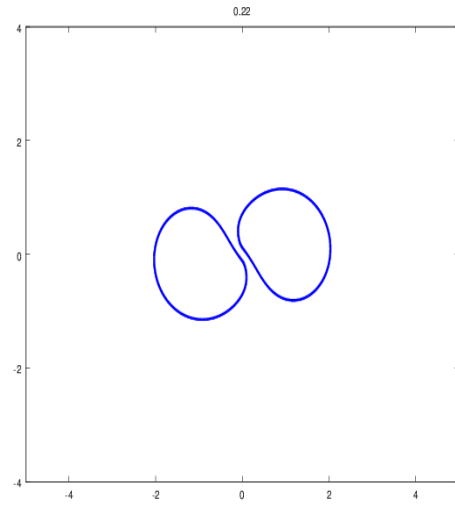
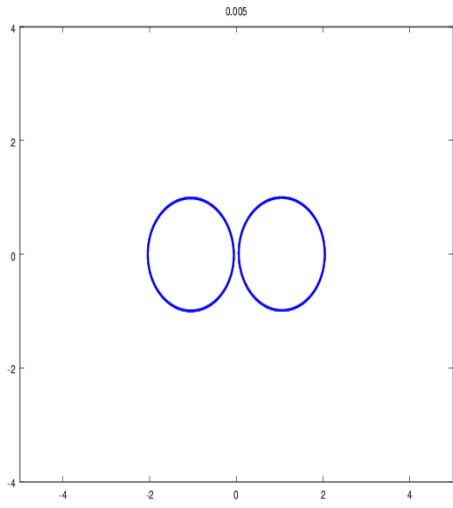


Figure 14: Interaction between circular VF and 2 point vortices

5.2 Interaction between VFs

The interaction between two circular VFs is investigated here. Two circular VFs of same strength and thickness are kept at a very small separation. The resulting interaction is shown above. Each VF rotates around the other, shears each other and sweeps thickness to a certain region which then starts to roll up. The spirals of roll up then merge together to form a complex pattern at the center. Rolling up is also initiated at other regions on the VFs.



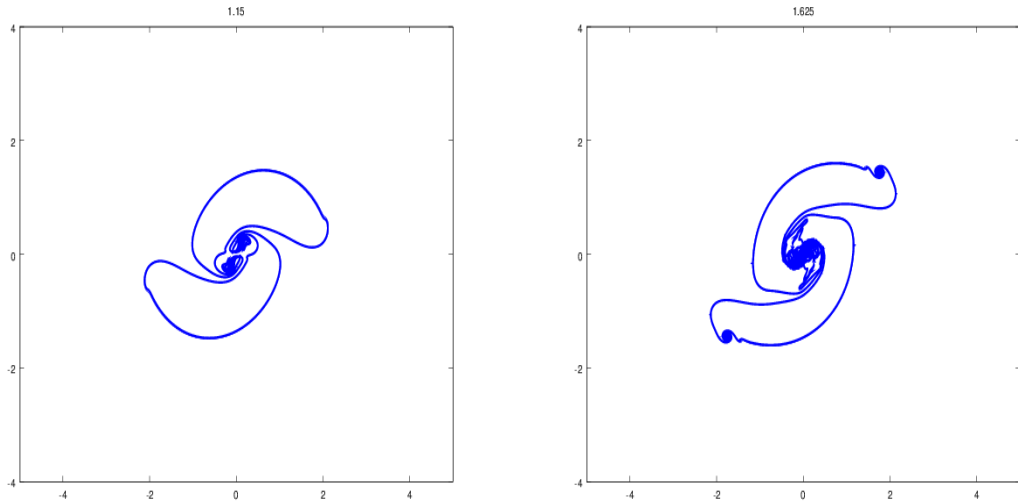


Figure 15: Interaction between 2 circular VFs

6 Conclusions

This work was undertaken with the goal of constructing a new reduction of the 2D Euler equations to model thin strips of vorticity or VFs. The new model (Filament Dynamics or FD) solves for a curve in the plane but has thickness slaved to it. Qualitative features of thin filaments such as rolling up and response to straining fields seems to be captured by the model. Comparisons with Contour Dynamics indicate similar behavior. Quantitative details and comparisons of instabilities in this model vs instabilities in the CD model remain to be examined.

CD often has difficulties capturing dynamics of very thin filaments, more so if the tips are sharp. CD tries to smooth the tips by adding in more points, taking up the role of viscosity. The number of points required also becomes larger with reduced thickness. These aspects force one to use techniques such as contour surgery[8]. As an application of the new model, one could imagine building a hybrid CD-FD code, where if the thickness of a certain strip reduces below a certain limit, the code would switch from CD to FD.

7 Acknowledgments

I would like to thank Philip Morrison for initial encouragement to pursue the idea when I first suggested this to him. His support throughout the work is gratefully acknowledged. Stephen Meacham was always available for discussions throughout the program and provided much fruitful advice. Glenn R. Flierl is thanked for the CD code used in this work and for many helpful suggestions.

8 References

1. McWilliams, J.C., The emergence of isolated, coherent vortices in turbulent flow. *J. Fluid Mech.*, 146 (1984), 21-43.
2. Kevlahan, N.K. and Farge, M., Vorticity filaments in two-dimensional turbulence: Creation, stability and effect. *J. Fluid Mech.*, 346 (1997) 4976
3. Katz, Joseph and Plotkin, Allen, *Low-Speed Aerodynamics*, Cambridge Aerospace Series (Book 13), 2001.
4. G. Birkhoff, Helmholtz and Taylor instability , *Proc. Symp. Appl. Math.*, XII , Amer. Math. Soc. (1962) pp. 5576
5. N. Rott, Diffraction of a weak shock with vortex generation. *J. Fluid Mech.*, 1 (1956) pp. 111
6. R. Krasny, Desingularization of periodic vortex sheet roll-up. *J. Comput. Phys.*, 65 (1986) pp. 292313
7. G. Kirchhoff, *Vorlesungen uber mathematische Physik, Mechanik*, Leipzig: Teubner, 1876.
8. D. Dritschel, Contour surgery: A topological reconnection scheme for extended integrations using contour dynamics. *J. Comp. Phys.*, 77 (1988) pp. 240-266.